Supporting Information

for

"Atomic Observation of Catalysis-Induced Nanopore Coarsening of Nanoporous Gold"

Takeshi Fujita,[1,2,*] Tomoharu Tokunaga,[3] Ling Zhang,[1] Dongwei Li, [4] Luyang Chen,[1] Shigeo Arai,[3] Yuta Yamamoto,[3] Akihiko Hirata,[1] Nobuo Tanaka,[3] Yi Ding,[4,*] and Mingwei Chen[1,5,6,*]

[1]Advanced Institute for Materials Research, Tohoku University, Sendai 980-8577, Japan

[2]PRESTO, JST, 4-1-8 Honcho Kawaguchi, Saitama 332-0012, Japan

[3]Ecotopia Science Institute, Nagoya University, Nagoya 464-8603, Japan

[4]Center for Advanced Energy Materials and Technology Research (AEMT), School of Chemistry and Chemical Engineering, Shandong University, Jinan 250100, PR China.

[5]State Key Laboratory of Metal Matrix Composites, School of Materials Science and Engineering, Shanghai Jiao Tong University, Shanghai 200030, PR China

[6]CREST, JST, 4-1-8 Honcho Kawaguchi, Saitama 332-0012, Japan

Supporting Movies

Movie S1. Observations before and after exposure to the CO/air gas mixture. After ~4 s, the sudden sample movement is caused by the opening of the gas valve to introduce the gas mixture. The video frequency is 25 fps.

Movie S2. Initial stage of nanopore coarsening after exposure to the CO/air gas mixture for ~50 seconds. All surface planes around the nanopore are faceted. The video frequency is 25 fps.

Movie S3. Sequence of nanopore coarsening during steady coarsening. The video frequency is 25 fps.

Movie S4. Twin planes as pinning sites slowing down the coarsening kinetics. The red arrows point to the twin planes and the {111} surface planes that subsequently diffused away. The video frequency is 25 fps.

Movie S5. Sequence of atomic motion on the surface. A few atoms have moved across the triple point in later frames, indicating that the layer-by-layer motion is associated with surface diffusion and not sublimation. The video frequency is 25 fps.

Table S1. Conversion percentages, CO reaction rates, and TOF values under different conditions in regard to the kinetics of NPG toward CO oxidation.[S1,S2] Apparently, increasing the O_2 concentration helps the reaction.

O_2 flow rate (mL)	CO:O_2 ratio	263 K			273 K		
		conv.[a]	R_{CO}[b]	TOF[C]	conv.[a]	R_{CO}[b]	TOF[C]
0.14	4:1	17.1	0.3	0.5			
0.28	2:1	22.5	0.5	0.7			
0.56	1:1	31.5	0.6	0.9	46.5	1.0	1.4
1.12	1:2	39.3	0.8	1.2	60.8	1.3	1.8
2.24	1:4	48.1	1.0	1.4	74.8	1.5	2.2
3.36	1:6	53.6	1.1	1.6	83.4	1.7	2.5
4.48	1:8	56.49	1.17	1.7	87.7	1.8	2.6
5.60	1:10	59.50	1.23	1.8	89.4	1.8	2.6
6.72	1:12	61.90	1.28	1.8	91.8	1.9	2.7
7.84	1:14	63.9	1.3	1.9	93.3	1.9	2.8
8.86	1:16	64.9	1.3	1.9	96.6	2.0	2.8
9.98	1:18	65.7	1.4	1.9	98.8	2.0	3.0

a:CO conversion (%); b:CO reaction rates(10^{-5} mol.g^{-1}.s^{-1}); c:TOF values (10^{-2} s^{-1})

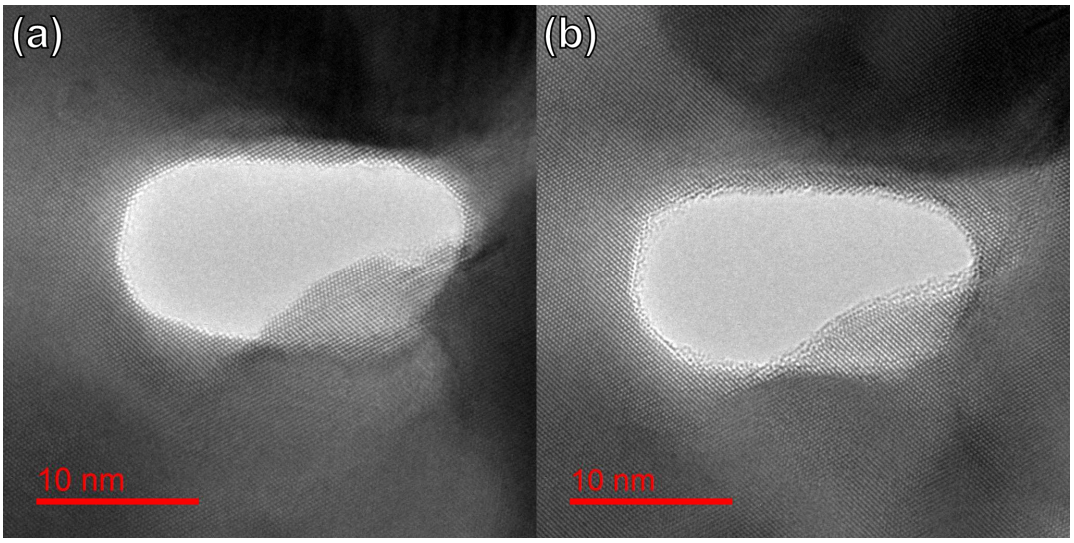

Figure S1. Structure stability under electron illumination in a pure N_2 environment at room temperature. The observation condition was described in the paper. The gas pressure was 30 Pa. (a) Initial structure and (b) structure after 3 min of electron illumination. The structure did not change within the similar time region as it did during *in situ* catalysis described in the paper.

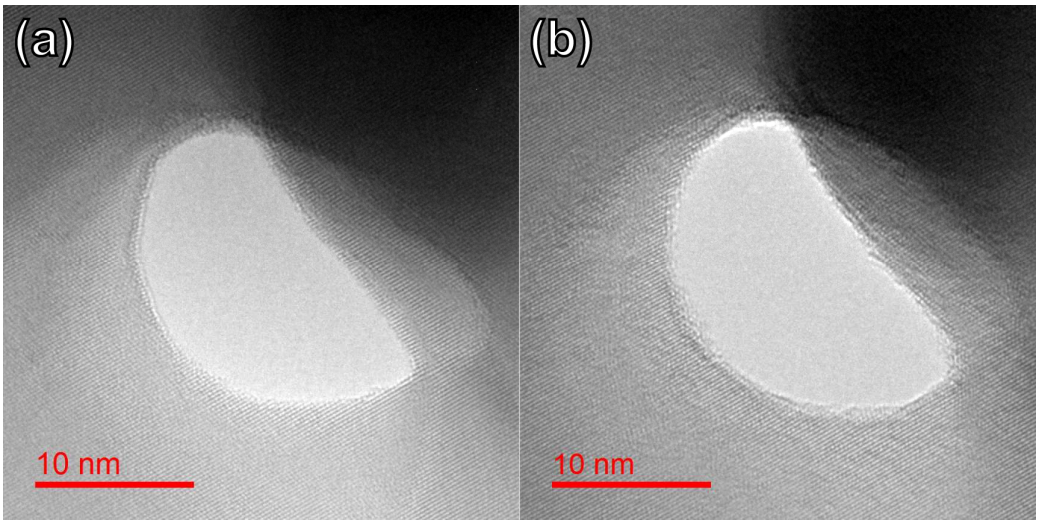

Figure S2. Structure stability under electron illumination in a pure O_2 environment at room temperature. The observation condition was described in the paper. The gas pressure was 6 Pa. (a) Initial structure and (b) structure after 3 min of electron illumination. The structure did not change within the similar time region as described in the paper.

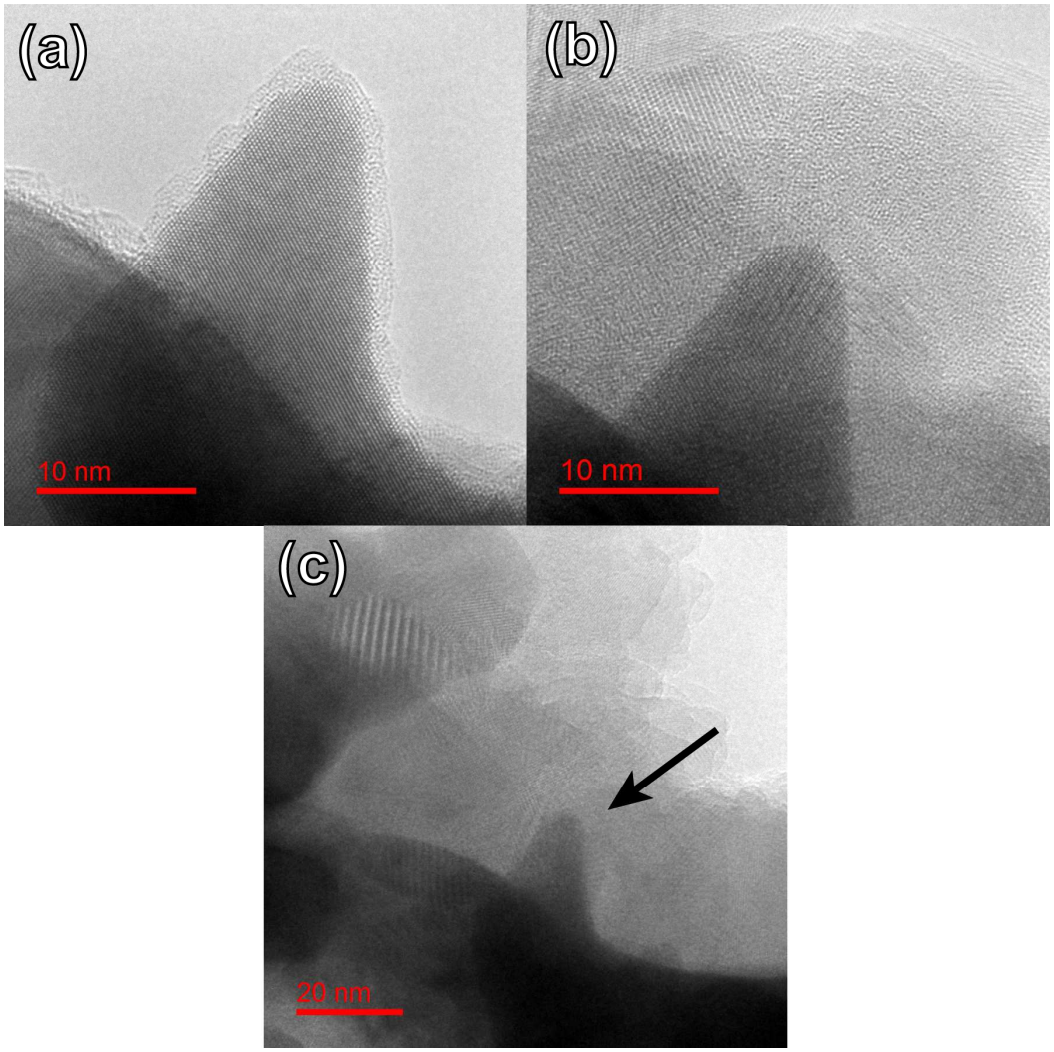

Figure S3. Structural stability under electron illumination in a pure CO environment at room temperature. The observation condition was described in the paper. The gas pressure was 10 Pa. (a) Initial structure, (b) structure after 75 seconds of electron illumination showing decomposition of CO to carbon ($CO = C + 1/2O_2$), and (c) structure after 2 min 30 s, showing that the areas of interest were completely buried in carbon, even though the initial structure remained intact.

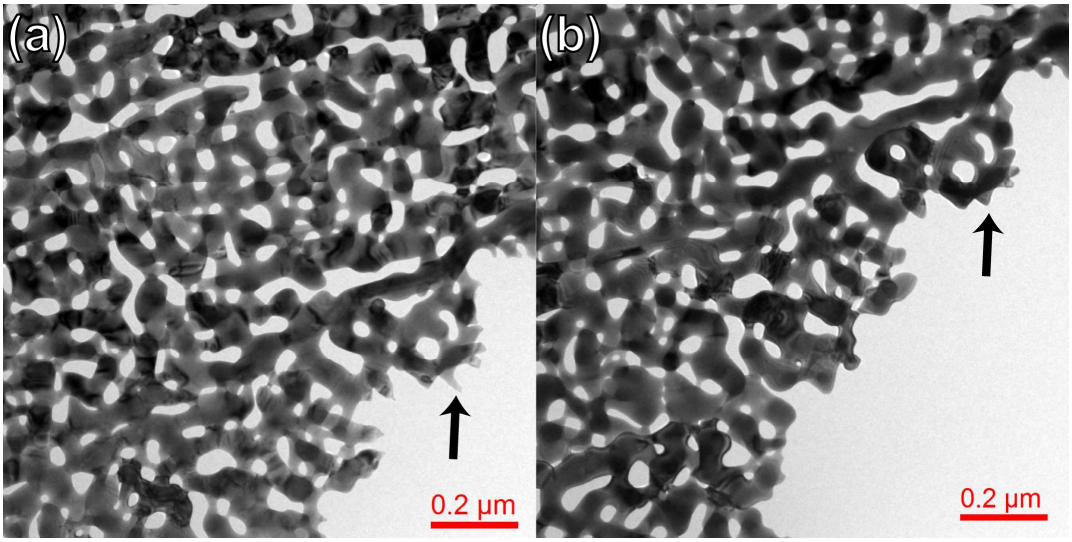

Figure S4. Structural stability upon thermal treatment at 300 °C in vacuum. (a) Initial structure and (b) structure after 5 minutes. The arrows in (a) and (b) show a ligament that was sharp in the beginning in (a), but became rounded in (b). However, the main structural feature did not change, indicating that NPG intrinsically has a high structural stability against pure thermal treatment.

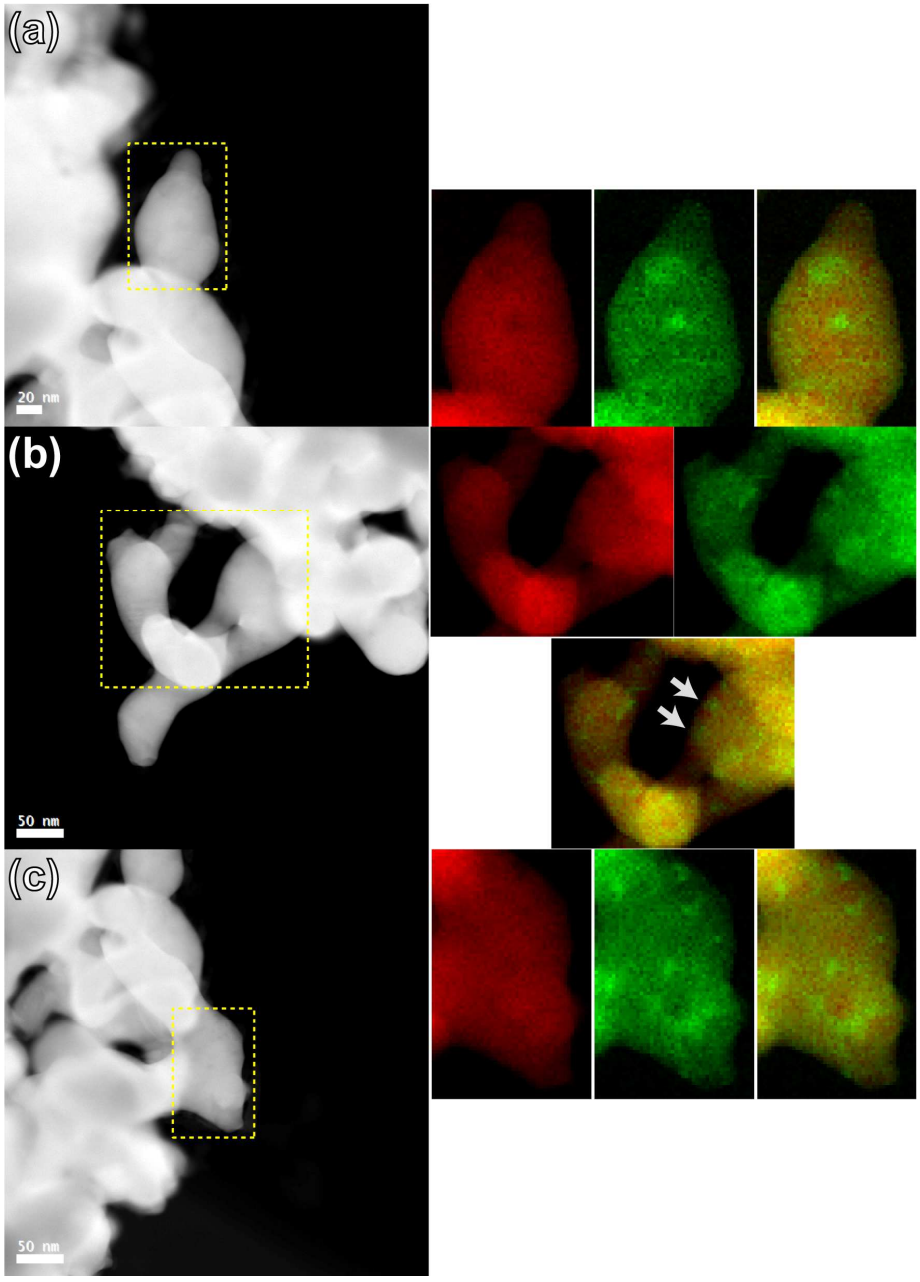

Figure S5. Three different areas of HAADF-STEM images of NPG at 70 % conversion and their corresponding EDS elemental mapping images. Au-L_α (in red), Ag-L_α (in green), and the corresponding mixed-color images from the selected areas. Arrows in (b) show segregated Ag atoms on the NPG surface.

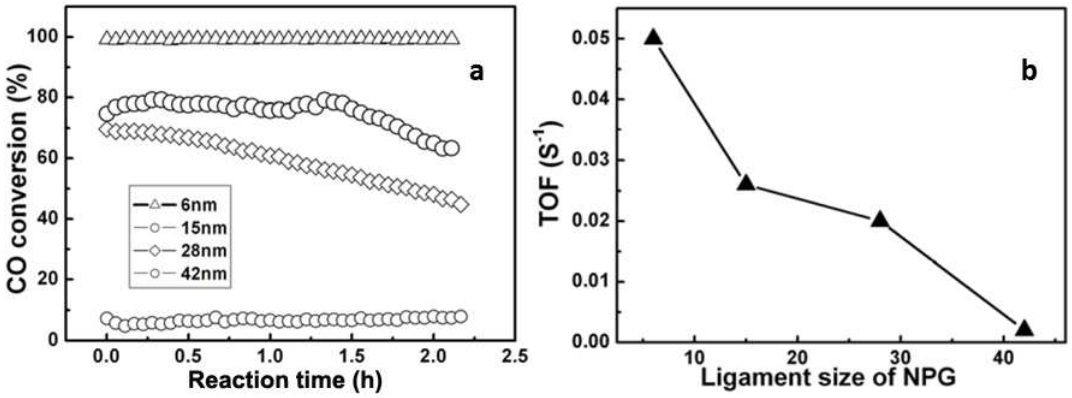

Figure S6. (a) CO oxidation activity and (b) and TOF values of NPG samples from ligaments of different sizes.[S1,S2] We had previously studied the CO oxidation activity of NPG samples of different ligament sizes, and had found that the activity decreased significantly when the ligament size was larger than 40 nm. By normalizing their activities to surface area, the thus-calculated TOF values also showed the same trend. The current *in situ* observations uncover the underlying mechanism of the size dependence. The coarsening of nanopores is accompanied by an increase in the number of surface facets and a decrease in the number of surface atomic steps that are the active sites for the catalytic reaction.

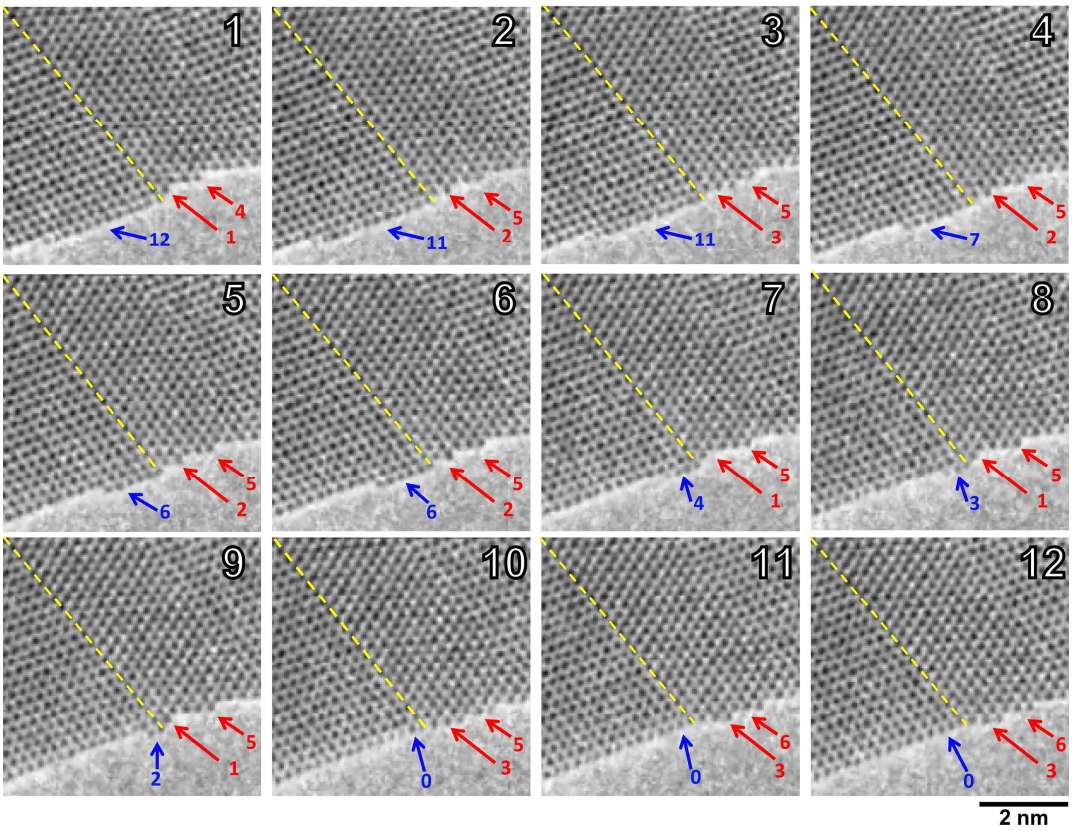

Figure S7. Sequence of captured images from 1 to 12 from the supplementary movie (**Movie S5**). Dotted lines represent the twin boundary. The blue numbers are the counted numbers of atoms located on the topmost surface. The red numbers are the counted numbers of atoms along the lines indicated by the arrows across the twin boundary (dotted line). It is clear that some of them are relocated on the surface across the twin boundary at the end.

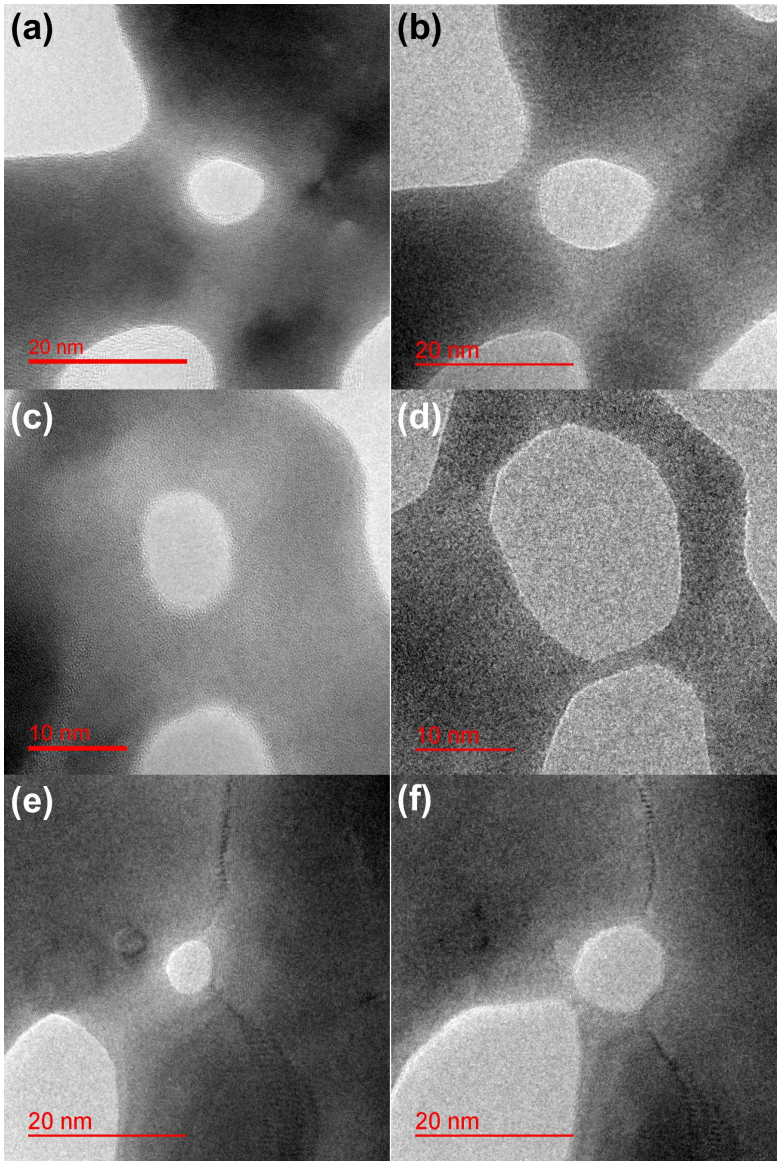

Figure S8. Observation, under a CO/gas mixture at 30 Pa at room temperature, of three nanopores located at a position not surrounded by twin planes. The observation condition is the same as that described in the paper. [(a), (c), (e)] Initial structure; (b) structure of (a) after 1 min; (d) structure of (c) after 75 seconds; (f) structure of (e) after 2 min 30 s. Each pore tends to grow isotropically, and the anisotropic growth by pinning of twins in Fig. 3 is obvious, as stated in the paper.

References

S1. Xu, C. X.; Su, J. X.; Xu, X. H.; Liu, P. P.; Zhao, H. J.; Tian, F.; Ding, Y. *J. Am. Chem. Soc.* **2007,** *129*, 42–43.

S2. Xu, C., Xu, X., Su, J. & Ding, Y. *J. Catal.* **2007**, *252*, 243–248.